



Published in final edited form as:

*Mol Oral Microbiol.* 2018 October ; 33(5): 364–377. doi:10.1111/omi.12238.

## Transcriptome Analysis of *Porphyromonas gingivalis* and *Acinetobacter baumannii* in Polymicrobial Communities

Daniel P. Miller<sup>1</sup>, Qian Wang<sup>1</sup>, Aaron Weinberg<sup>2</sup>, and Richard J. Lamont<sup>1,\*</sup>

<sup>1</sup>Department of Oral Immunology and Infectious Diseases, University of Louisville School of Dentistry, Louisville KY 40241, USA

<sup>2</sup>Department of Biological Sciences, Case Western Reserve University, Cleveland, OH 44106, USA

### Summary

*Acinetobacter baumannii* is a nosocomial, opportunistic pathogen that causes several serious conditions such as meningitis, septicemia, endocarditis and pneumonia. It can be found in the oral biofilm, which may be a reservoir for pneumonia and chronic obstructive pulmonary disease. Subgingival colonization by *A. baumannii* is associated with chronic and aggressive periodontitis as well as refractory periodontal disease. *Porphyromonas gingivalis*, a keystone periodontal pathogen localized to subgingival plaque, is also implicated in several chronic conditions including aspiration pneumonia. While both bacteria are found together in subgingival plaque and can cause multiple polymicrobial infections, nothing is known about the interactions between these two important human pathogens. In this study, we used RNA sequencing to understand the transcriptional response of both species as they adapt to heterotypic communities. Among the differentially regulated genes were those encoding a number of important virulence factors for both species including adhesion, biofilm formation, and protein secretion. Additionally, the presence of *A. baumannii* increased the abundance of *P. gingivalis* in model dual species communities. Collectively these results suggest that both *P. gingivalis* and *A. baumannii* adapt to each other and have synergistic potential for increased pathogenicity. In identifying the mechanisms that promote pathogenicity and refractory disease, novel approaches to mitigate polymicrobial synergistic interactions may be developed to treat or prevent associated diseases.

### Keywords

*Porphyromonas gingivalis*; *Acinetobacter baumannii*; RNA-seq; heterotypic communities

### Introduction

Studies of the human microbiome have enhanced our understanding of polymicrobial communities and the interactions among organisms. Periodontal diseases arise from

\*For correspondence: Richard J. Lamont, 570 South Preston Street, University of Louisville, Louisville, KY, 40202, Phone: 502-852-2112, Fax: 502 852 6394, rich.lamont@louisville.edu.  
DR DANIEL MILLER (Orcid ID : 0000-0002-1332-5870)  
DR RICHARD J LAMONT (Orcid ID : 0000-0002-3147-5039)

synergistic polymicrobial interactions between members of the oral community that result in dysbiosis and destructive inflammation<sup>1-4</sup>. The oral microbial community develops in a highly programmed process as early colonizers, predominantly Gram-positive facultative organisms such as the oral streptococci, adhere to mucosal and solid surfaces<sup>5,6</sup>, and then provide a substratum for attachment of later colonizers while also providing nutrient and physiological support. *Porphyromonas gingivalis* (*Pg*) is a Gram-negative late colonizer of oral biofilms. *Pg* has long been linked with periodontal diseases, but more recently has been associated with several severe conditions such as atherosclerosis, rheumatoid arthritis, respiratory infections and oral cancer<sup>7-11</sup>.

In the oral microbiome, in addition to classically defined periodontal pathogens, newly identified species and other medically relevant pathogens such as *Pseudomonas aeruginosa*, *Klebsiella pneumoniae*, and *Acinetobacter baumannii* (*Ab*) are being recognized<sup>12,13</sup>. *Ab* causes a variety of serious infections including pneumonia, urinary tract infections, endocarditis and skin and/or wound infections. While the role of *Ab* in periodontal disease is unknown and its interactions with other organisms within the oral microbial community are largely unstudied, it is often associated with anaerobic late colonizers. This is potentially due to antagonistic interactions with the early colonizer *Streptococcus sanguinis* that inhibits *Ab* growth<sup>14</sup>. The presence of *Ab* with classical periodontal pathogens such as *Pg*, *Treponema denticola*, *Aggregatibacter actinomycetemcomitans*, and *Tannerella forsythia* is associated with aggressive and chronic periodontitis<sup>15-18</sup>. Additionally, patients suffering from periodontitis are also more likely to be refractory to treatment if *Ab* is present<sup>19,20</sup>.

While there is a lack of evidence showing a causal relationship between periodontal and pulmonary diseases, oral plaque has been suggested as a reservoir for potential respiratory pathogens, and aspiration of these bacteria can lead to pneumonia<sup>21</sup>. Moreover, several studies have shown that the severity of periodontal disease is linked to adverse respiratory conditions. A study of elderly patients with periodontitis demonstrated that > 4 mm probing depth in at least 10 teeth was associated with an increased mortality due to pneumonia. Additionally, decreased periodontal ligament attachment and increased alveolar bone loss, two hallmark clinical manifestations of periodontitis, have been linked to reduced pulmonary function<sup>22-24</sup>.

Beyond periodontitis, specific periodontal pathogens may contribute to the etiology of respiratory diseases. Common periodontal pathogens *Fusobacterium nucleatum* and *Bacteroides spp.* (since re-classified as *Pg* and *Prevotella intermedia*) have been isolated from patients with aspiration pneumonia and lung abscesses<sup>25-27</sup>. Synergistic polymicrobial interactions involving oral bacteria have also been demonstrated for respiratory diseases. Mixed infections of *Pg* and *T. denticola* in a pneumonia mouse model caused more severe bronchopneumonia and increased mortality compared to mono-infections<sup>28</sup>. The bronchial clearance of *Pg* was delayed in the presence of *T. denticola*, and pro-inflammatory cytokines were increased in mixed infections. Polymicrobial infections of oral pathogens *Pg*, *F. nucleatum* or *A. actinomycetemcomitans* increased the invasion of *P. aeruginosa* into HEp-2 cells, stimulated greater cytokine production and elevated apoptotic cell death compared to infection with *P. aeruginosa* alone<sup>29</sup>. The commensal oral bacterial species *Actinomyces naeslundii* and *Streptococcus gordonii* did not affect *P. aeruginosa* invasion. Collectively

these studies suggest that oral pathogens can either directly infect the lower respiratory system or synergistically influence respiratory pathogens and enhance disease.

As *Pg* and *Ab* can be located together in the oral biofilm, study of their polymicrobial communities and interspecies interactions may begin to illuminate their contributions to the etiology of both periodontal and respiratory diseases. Here, we have used RNA sequencing (RNA-Seq) to study the transcriptional response of *Pg* and *Ab* in a model community. The results provide novel insight into the physiological response and the potential synergistic interactions between *Pg* and *Ab*.

## Materials and Methods

### Bacterial strains and growth conditions

*Porphyromonas gingivalis* (*Pg*) ATCC 33277 was grown anaerobically in trypticase soy broth (TSB) supplemented with 1 mg/mL yeast extract, 5 ug/ml hemin and 1 ug/ml menadione. TSB broth was supplemented with 5% sheep blood and 5% agar for growth on solid media. *Acinetobacter baumannii* (*Ab*) AB0057 was grown aerobically in Brain Heart Infusion (BHI) broth or BHI agar plates.

### Community Development

Polymicrobial communities for sequencing were generated as previously described<sup>30</sup>.  $1 \times 10^9$  cells of *Pg* and *Ab* were pelleted by centrifugation and resuspended in phosphate buffered saline (PBS). The two species were then mixed, pelleted and held aerobically at 37C for 3 h. Control *Pg* and *Ab* cells alone were prepared under the same conditions.

### RNA Purification, Sequencing and Analysis

Total RNA was isolated from the cells using the Qiagen RNAeasy kit (Qiagen) with DNase treatment. Ribosomal RNA depletion was performed using the Ribo-zero rRNA removal kit for bacteria (Illumina) and the libraries were constructed with the TruSeq mRNA library kit (Illumina). High throughput sequencing was performed on a HiSeq 2500v.4 (Illumina) at the University of Michigan Medical School Sequencing Core. Reads were mapped to the reference genomes from NCBI for *A. baumannii* AB0057<sup>31</sup> and *P. gingivalis* ATCC 33277<sup>32</sup>. Normalized read counts and p-values for differential expression were computed for four biological replicates. The p-values were corrected for multiple hypothesis testing using the q-value method<sup>33,34</sup>. Transcripts with an absolute  $\log_2$  fold difference of greater than 0.5 and the q-value below 0.001 were considered statistically different. Data processing and analysis for differential expression was performed by the University of Michigan Bioinformatics core. All sequencing reads and analyzed data were deposited to the Gene Expression Omnibus (GEO, accession number GSE111038). Topological pathway analysis was performed using the Bioconductor software package which takes into account the position of the differentially expressed genes in the pathway map from the Kyoto Encyclopedia of Genes and Genomes (KEGG)<sup>35</sup>. Pathways were identified as significantly regulated when the false-discovery rate was  $<0.05$ .

## Quantitative Reverse Transcriptase-PCR Validation

To validate the RNA sequencing results, expression of select genes was determined by qRT-PCR. *Pg*, *Ab* and *PgAb* communities were developed and RNA isolated as described above. RNA was isolated from three independent experiments and converted to cDNA using the High Capacity cDNA Reverse Transcription kit (Applied Biosystems). qRT-PCR was performed by StepOne Plus (Applied Biosystems) using the  $C_t$  method using 16s rRNA as an internal control. Primers used for qRT-PCR are described in Supplemental Table 1.

## Heterotypic Community Development and Confocal Microscopy

Communities of *Pg* and *Ab* were generated essentially as described previously<sup>36</sup>. *Ab* cells (0.1 OD<sub>600</sub>) were stained with Texas Red in PBS for 30 min and coated on glass coverslips for 24 h aerobically at 37°C. *P. gingivalis* cells were labeled with FITC and reacted with *Ab* in PBS for 16 h aerobically 37°C. After washing, the coverslips were mounted to glass microscope slides and examined using a Leica SP8 confocal microscope using 488 nm (FITC) and 558 nm (Texas Red) lasers. XYZ stacks were digitally reconstructed and quantification of volume of each species was obtained using the Find Objects algorithm in the Volocity software. The images are representative of at least 3 experiments and the quantification is the average of 6 measurements from each biological replicate.

## Results and Discussion

Transcripts from mixed communities of *P. gingivalis* (*Pg*) and *A. baumannii* (*Ab*) following three hours of aerobic co-incubation were analyzed to identify differentially expressed genes compared to both bacterial species in monoculture. Our previous analysis of the transcriptional response of *Pg* to *S. gordonii* (*Sg*) over-time revealed the most consistent transcriptional changes occurred between 2 and 6 hours of co-incubation<sup>37</sup>. Additionally, our incubation was conducted under aerobic conditions as *Ab* is a strict aerobe and *Pg* is an aerotolerant anaerobe with resistance to aerobic conditions for 5 hours<sup>38</sup>. Based on these previous finding, we selected a 3 hour incubation under aerobic conditions for our experiment. A total of 12 libraries, 4 biological replicates each from *Pg* and *Ab* alone and the dual species communities (*PgAb*) were prepared and sequenced using Illumina technology. The complete data sets are shown in Supplemental Table 2. Genes were determined to be differentially expressed in communities when transcripts with an absolute log<sub>2</sub> fold difference of greater than 0.5 were identified compared to the mono-species controls and the q-value below 0.001 were considered statistically different. A comparison of gene expression levels between *Pg* and *PgAb* communities revealed 713 genes (34.1% of protein coding genes) were differentially expressed, and of those, 351 genes had increased transcript levels in mixed communities while 362 genes had reduced expression in the *PgAb* communities. Pathway analysis using Kyoto Encyclopedia of Genes and Genomes (KEGG) was attempted for the *Pg* vs *PgAb* data; however, no pathways were determined to be significant, likely due to over representation of genes encoding hypothetical proteins (discussed below). Changes in the *Ab* transcriptional program in the context of dual-species communities were also assessed. There were 1676 differentially expressed genes (44.1% of protein coding genes), with 847 of these up-regulated, and 829 down-regulated, in *PgAb* compared to *Ab*. Representative genes were selected for qRT-PCR validation of *Ab* genes

and the results are shown in Supplemental Table 3. Pathway analysis identified 24 pathways of *Ab* that were significantly regulated in the mixed communities compared to single species communities (Table 1). The largest group, made up of 68 genes, related to purine metabolism. Many genes were also involved in peptidoglycan biosynthesis, propionate, pyruvate, and sulfur metabolism. This indicates that *Ab* is more physiologically active in the *PgAb* communities compared to *Ab* alone. As no exogenous nutrients were provided in the communities, these results suggest significant cross-feeding between *Pg* and *Ab*. While it is likely that incubation under aerobic conditions could influence the transcriptional landscape of *Pg*, it is likely that *Pg*, an aerotolerant organism at the leading edge of the subgingival community, will encounter higher oxygen environments when interacting with *Ab*, a strict aerobe.

Figure 1 graphically represents the  $\log_2$  fold change for every open reading frame from *PgAb* compared to *Pg* and *Ab*, respectively. For the *PgAb* vs *Pg* data set, a large portion of differentially expressed genes are annotated as hypothetical proteins (34.1%). Multiple large clusters of genes annotated as hypothetical proteins were differentially expressed and several were very highly regulated. Studies are ongoing to assess the function of these proteins. For the *PgAb* vs *Ab* data set, a number of functional clusters that were identified in the pathway analysis are highlighted. These include genes involved in sulfur metabolism which were negatively regulated by *Ab* in response to *Pg*. Multiple clusters of genes identified in purine metabolism are also highlighted. Genes of known functional and pathogenic significance were further analyzed and are described below.

### Phenylacetic acid catabolism

The Phenylacetic Acid Catabolism (PAA) pathway is encoded by the *paa* operon (AB57\_1518 – AB57\_1530) and is essential for the catabolism of several aromatic compounds such as phenylacetate, and yields acetyl- and succinyl-CoA, utilized by the TCA cycle<sup>39</sup>. The PAA pathway of *Ab* as well as other pathogens is associated with virulence and modulation of neutrophil chemotaxis<sup>40,41</sup>. PaaABCDE form a multi-protein complex that is most closely associated with virulence through production of toxic epoxides. Expression of the later genes in the *paa* pathway, *paaZ*, *paaG*, *paaJ*, and *paaH* were all significantly higher in the *PgAb* community compared to *Ab* alone (Figure 2), suggesting that *Ab* may produce more acetyl-CoA and succinyl-CoA in response to *Pg*. The increased production of both may feed into the TCA cycle for energy generation. Alternatively, increased succinyl-CoA production by the PAA pathway may be utilized by *Pg*. Similarly, *Pg* has been shown to induce succinate biosynthesis and secretion in *T. denticola* for cross-feeding<sup>42</sup>. While *Pg* lacks a PAA pathway, it does retain a *paaK* homolog (PGN\_0228) which was up-regulated in communities with *Ab*. PaaK catalyzes the conversion of phenylacetate to phenylacetyl-CoA (PA-CoA), a terminal product for *Pg*. PA-CoA was shown to be the inducer of the PAA pathway in *Pseudomonas putida*<sup>43</sup>. Hence, *Pg* may synthesize PA-CoA which in turn stimulates the PAA pathway of *Ab* and lead to increased levels of acetyl-CoA and succinyl-CoA. Beyond the potential for metabolic cross-feeding, increased catabolism of phenylacetate may result in decreased neutrophil chemotaxis as phenylacetate from *Ab* is a neutrophil chemoattractant<sup>40</sup>. Such a process could link nutritional cross-feeding with polymicrobial synergy in *PgAb* communities.

## Expression of adhesins in *PgAb* communities

Colonization of the oral cavity and development of the polymicrobial biofilm involves attachment to both biotic and abiotic surfaces. *Pg* produces a number of adhesins such as the FimA and Mfa1 fimbriae along with the accessory proteins (FimB-FimE and Mfa2-Mfa5 respectively), and hemagglutinin A (HagA), HagB and HagC<sup>44</sup>. FimA and HagA were two of top 10 most negatively regulated *Pg* genes in the *PgAb* community. The expression of the long fimbriae major subunit FimA along with accessory genes PGN\_0181 and PGN\_0182 (the two fragments of FimB in 33277), FimC, FimD and FimE were all reduced in the *PgAb* communities compared to *Pg* alone (Figure 3). FimA fimbriae mediate attachment to diverse substrates such as other oral bacteria, the gingival epithelium and matrix proteins<sup>45,46</sup>. Expression of the hemagglutinin protein HagA was significantly decreased in the *PgAb* community compared to *Pg* alone, while expression of the structurally and functionally distinct HagB/C proteins was unchanged. HagA is a large protein composed of multiple repeating domains that each possess hemagglutinin activity, and is involved in attachment to endothelial and epithelial cells<sup>47</sup>.

The Mfa1 fimbriae accessory Mfa3-5 transcripts were higher in the *PgAb* community compared to *Pg* alone, while Mfa1 and Mfa2 were unchanged. Mfa1 is the structural fimbrial subunit while Mfa2 acts as an anchor and regulates filament length. Mfa3-5 are located along the fimbrial structure and have been shown to be co-expressed as an operon with Mfa1-2<sup>48</sup>. Mfa3 is localized to the fimbrial tip and is essential for the Mfa4 and Mfa5 integration into the mature fimbriae<sup>49</sup>. Post-transcriptional regulation of Mfa3-5 may modulate the expression of the accessory proteins independently from *mfa1*. These findings are supported by our previous analysis of the transcriptional response of *Pg* to *Streptococcus gordonii*<sup>37</sup>. In both studies, detailed analysis of the reads mapped to the *mfa* operon reveal that *mfa1* expression is detached from the downstream *mfa2-5* genes. These differences may be due to inter-operon transcriptional start sites, differences in mRNA stability or transcriptional attenuation. Additional studies in our laboratory are exploring the role of Mfa2-5 in heterotypic communities. Collectively, these results indicate that *P. gingivalis* can dispense with the production of energetically costly adhesin proteins after community development is initiated, although Mfa3-5 may play specialized roles.

*Ab* encodes 4 distinct type 1 pili, 3 of which were differentially expressed in the polymicrobial community<sup>50</sup>. The first gene cluster comprising AB57\_1744 through AB57\_1747 was unchanged compared to *Ab* alone (Figure 3). This fimbrial cluster has been shown to be up-regulated in biofilm cells versus planktonic growth but a direct involvement in biofilm formation has not been established<sup>51</sup>. This cluster was also found to be down-regulated under iron limited conditions<sup>52</sup>. The type 1 pilus produced by the CsuA/BABCDE usher-chaperone assembly system is essential for initial biofilm development by attaching to abiotic surfaces and mediating early biofilm development<sup>51,53</sup>. These pili have additionally been shown to mediate attachment to alveolar epithelial cells and *Candida albicans*<sup>54</sup>. The major pilin subunit CsuA/B and the accessory CsuB,C,D transcripts were significantly up-regulated in the *PgAb* community versus *Ab* alone. A second usher-chaperone assembly system (AB57\_2003 – AB57\_2007) encodes type 1 pili, termed p-pili, that are also involved in biofilm and pellicle formation<sup>55</sup>. AB57\_2007, encoding the fimbrial subunit, was

increased in the *PgAb* community along with all other genes in the operon except AB57\_2003. The putative type 3 filamentous fimbriae composed of FilABCDEF (AB57\_0739 – AB57\_0744) is up-regulated in biofilm pellicle compared to planktonic cells<sup>55</sup>. The genes encoding FilB, FilE and FilF were significantly decreased in response to *Pg* compared to untreated *Ab*. These data suggest that the CsuA/B pili and the p-pili are involved in heterotypic community maintenance while the FilA fimbriae may be dispensable following initial community development. In addition to polymicrobial community development, increased adhesion expression may be important for binding to oral epithelial cells and is the subject of future investigation.

### Type VI secretion

Type VI secretion systems (T6SS) are analogous to bacteriophage contractile tail assemblies that mediate the injection of effectors into target cells<sup>56</sup>. T6SS effectors can be toxic to both bacteria and eukaryotic cells. The T6SS of *Ab* is encoded by a 20 gene cluster and has been shown to kill *E. coli*, suggesting this system may function for bacterial competition<sup>57</sup>. The T6SS genes are highly conserved among *Ab* isolates, and although not all *Ab* strains produce an operational T6SS<sup>58</sup>, AB0057 has been shown to produce a functional system<sup>59</sup>. Several of the T6SS machinery genes as well as T6SS effectors were differentially expressed in *PgAb* (Table 2) compared to *Ab* alone. TssB along with TssC assemble into cytoplasmic structures resembling bacteriophage sheaths that extend and contract<sup>60</sup>. Assembly of the TssB/C sheath is also dependent upon the gp25-like protein, TssE. TagX is a peptidoglycan hydrolase and is an essential enzyme in allowing transit of the T6SS machinery through the *Ab* peptidoglycan<sup>61</sup>. The T6SS leads to the export of two hallmark effector proteins, Hcp and VgrG<sup>60</sup>. Hcp forms hexameric rings and is homologous to the phage protein gpV. The presence of Hcp in the supernatant of T6SS encoding organisms is evidence for a functional secretion system. Hcp and VgrG are usually co-dependent for export. TssM, TssB, and Hcp have all been shown to be essential for *Ab* pathogenicity in a murine septicemia model<sup>58</sup>. The *PgAb* community showed increased levels of the *tssB*, *tssC*, and *tssE* along with *tagX*. AB0057 encodes three putative VgrG-like proteins one of which was differentially expressed, along with Hcp, in response to *Pg*. Additional genes within the operon were also up-regulated whose function within the T6SS are yet to be determined. In order to determine if the T6SS of AB0057 kills *Pg*, the *PgAb* community was incubated for three hours and *Pg* cells were then plated to determine CFU counts. There was no change in CFU when *Pg* was incubated alone or with AB0057 suggesting the T6SS is not lethal to *Pg* (data not shown). The ability to regulate the T6SS in the context of a complex polymicrobial community may alter the microbial community by favoring those resistant to T6SS-mediated killing such as *Pg*. In other Gram-negative bacteria, T6SS have been shown to be involved in metal acquisition such as iron<sup>62</sup> as well as quorum sensing and biofilm formation<sup>63</sup>. In some bacteria, T6SS and effectors target eukaryotic cells and are required for virulence<sup>64,65</sup>. While the exact role the *Ab* T6SS plays in polymicrobial communities is unknown, the up-regulation may enhance *Ab* virulence by bactericidal-independent functions. Additionally, *Pg* induction of the *Ab* T6SS activity may lead to effector mediated killing of sensitive subgingival community members and alter the polymicrobial constituents.

## Type IX Secretion

*Pg* produces a type 9 secretion system (T9SS) for the movement of proteins across the outer membrane<sup>66</sup>. Currently over 30 proteins that contain a conserved C-terminal domain (CTD), that is required for secretion, are transported through the T9SS. Genes encoding the core machinery of the T9SS are scattered across the *Pg* genome with the exception of the *porKLMN* operon. The transcript levels for the *porKLMN* operon were increased in the *PgAb* community (Table 3). Additional T9SS machinery genes *sov*, *porU*, *porV*, and *porZ* were also significantly up-regulated in response to *Ab*. The T9SS is regulated by the two-component system proteins PorX and PorY that functions through the transcriptional regulator SigP<sup>67</sup>. While neither the histidine kinase nor the response regulator were differentially expressed, transcript of SigP which has been shown to directly interact with the *porKLMN* promoter was increased<sup>68</sup>. A number of important virulence-associated proteins such as peptidylarginine deiminase (PPAD) and the gingipains are secreted through the T9SS<sup>66</sup>. Increased levels of the T9SS components may contribute to more significant virulence in the *PgAb* community compared to *Pg*. In addition to the core T9SS, 20 of the 30 T9SS secreted proteins also showed differential expression; 11 were up-regulated and 9 down-regulated (Table 3). PPAD and the arginine specific gingipain RgpB are two potential virulence factors that had the highest degree of up-regulation<sup>68-71</sup>. C5a citrullination by PPAD has been shown to reduce neutrophil chemotaxis<sup>72</sup>, suggesting a second potential mechanism of synergistic neutrophil manipulation by *Pg* and *Ab* in addition to phenylacetate metabolism and could be the focus of future studies.

## Proteases

*P. gingivalis* is an asaccharolytic organism that relies on proteolysis to reduce proteins to peptides that serve as carbon and nitrogen sources<sup>44</sup>. A class of cysteine proteases, the gingipains, are important virulence factors<sup>73</sup>, and gingipains are specific for either arginine (RgpA/B) or lysine (Kgp). In addition to nutrient acquisition, gingipains are also involved in processing of surface proteins and degradation of host proteins. The gingipains degrade host immune proteins and can be released intracellularly and degrade host signaling proteins<sup>68,74,75</sup>. In our heterotypic communities, only RgpB was significantly up-regulated while RgpA and Kgp were not differentially expressed (Table 3). PrtT, a trypsin-like protease that is linked to virulence in a mouse abscess model<sup>76</sup> was also up-regulated in the *PgAb* community.

## Tetratricopeptide Repeat (TPR) Domain Proteins

The TPR domain is a protein-protein binding motif that is often repeated within functionally diverse proteins. In *Pg*, genetic deletion of *tprA* (PGN\_0876) was shown to reduce virulence in a mouse abscess infection model<sup>77</sup>. *tprA* was up-regulated in the heterotypic community compared to *Pg* alone (Figure 4). Among the other TPR proteins, PGN\_0996 and PGN\_1323 were also increased in response to *Ab* while PGN\_0972 was reduced. In *Ab*, AB57\_0888 is a TPR-domain containing lipoprotein that is annotated as a DNA uptake protein as part of the competence system, and this gene is increased in response to *Pg*. Collectively these data suggest that *Pg* may be more virulent in response to *Ab*, while *Ab*



can up-regulate its DNA uptake system which provides an advantage in a competitive polymicrobial environment.

### **A. baumannii capsule biosynthesis**

Capsules are essential virulence factors in numerous bacterial species. *Ab* isolates produce at least 6 different capsule types with the enzymes involved in biosynthesis of sugar precursors and surface polysaccharide transferases being the most variable in gene arrangement<sup>78</sup>. Nearly every strain possesses a capsule encoded locus, including AB0057 used in this study (AB57\_0090 - AB57\_0116). Within this locus 10/27 genes were significantly up-regulated in the heterotypic community compared to *Ab* alone (Table 4), including the tyrosine kinase (AB57\_0091) and the *wza* gene (AB57\_0093) which have been shown to be essential for capsule production<sup>79</sup>. Genetic deletion of either gene results in increased sensitivity to human serum and decreased virulence in a murine subcutaneous infection model<sup>79</sup>. In addition to the capsule locus, AB57\_1078 encodes a *wzi* homolog that in other bacteria has been shown to be essential for attachment of the capsule to the outer membrane<sup>80</sup>. These data suggest that *Ab* may increase capsule biosynthesis in the presence of *Pg*, which would make *Ab* more resistant to innate immune killing mechanisms and more virulent.

### **Iron acquisition by *Pg***

Iron is essential for the growth and survival of bacteria and the human host as this critical metal is required as a cofactor for many essential enzymes involved in cellular and metabolic processes. In the host, iron is tightly sequestered by ferritin, lactoferrin and transferrin to protect against oxidative damage by the Fenton reaction. Acquisition of iron is an essential survival and virulence trait of all successful pathogens.

*Pg* growth is dependent upon iron acquisition in the form of hemin<sup>81,82</sup>. Interestingly the regulation of iron acquisition related genes within our heterotypic communities was variable (Table 5). The *hmuYRSTUV* operon encodes a hemin binding protein HmuY and the membrane bound receptor HmuR. The operon contains 4 of the 10 most positively regulated genes in the *PgAb* community. Consistent with increased need for iron acquisition, ferritin transcript levels were reduced indicating reduced need for iron storage. Additionally, PGN\_1058 (bacterioferritin comigratory protein, *bcp*), which has previously been shown to be down-regulated during iron-limited conditions<sup>83</sup> was significantly reduced in the *PgAb* community. In contrast, mRNA for the TonB-linked receptor, Tlr, and HtrABCD which comprise an ABC transport system involved in hemin acquisition<sup>84</sup>, were strongly reduced in the *PgAb* community. Additional hemin uptake systems encoded by the *ihf*<sup>85</sup> and *hus*<sup>86</sup> operons were not differentially expressed in the *PgAb* communities. HaeR/S is a two-component system (TCS) that regulates iron acquisition<sup>83</sup>. Both HaeR and HaeS showed reduced expression in the *PgAb* community, however only HaeR was determined to be significant due to a q-value that did not meet our strict significance cut-off for HaeS. HaeR was demonstrated to act as both an activator and repressor depending on promoter binding and hemin concentration. Interestingly HaeR has also been shown to regulate the *hmu* operon, *htrA* and *bcp*, suggesting that all differentially expressed genes in response to *Ab* may be through HaeR<sup>83</sup>, although transcript levels for TCS do not necessarily reflect activation status and information flow.

## Dual-species community development

Both *Pg* and *Ab* are biofilm producing organisms that can be found as part of complex polymicrobial communities during infection. The RNA-Seq data revealed transcriptional responses in both *Pg* and *Ab* adhesins associated with biofilm formation in the mixed communities compared to mono-species biofilms. In a dual species community model we found the abundance of *Pg* was significantly increased in the presence of *Ab* compared to monotypic conditions (Figure 5). These data demonstrate that the transcriptional changes highlighted in the RNA-Seq communities can lead to increased heterotypic community development.

## Comparison of heterotypic community responses

*P. gingivalis* thrives in a complex polymicrobial environment. Numerous studies have shown that *Pg* synergistically interacts with various members of the subgingival microbiome. One of the best characterized is the relationship between *Pg* and *S. gordonii* (*Sg*), including our recent analysis of the *Pg* transcriptional response to *Sg* by time-coursed RNA-Seq<sup>37</sup>. Comparing the transcriptional responses of *Pg* to *Ab* and *Sg* may provide insight into common responses to polymicrobial environments or highlight species-specific responses. One key difference between these two studies was the expression of fimbriae by *Pg*. *PgSg* communities resulted in significant increases in FimA and Mfa1 fimbrial expression over-time whereas in this study, the overall adhesive genes of *Pg* were down-regulated. This suggests that while *Pg* can directly interact with both *Sg* and *Ab*, *Sg* may provide prolonged stimuli for heterotypic community maintenance, whereas following initial community formation with *Ab* the fimbriae are no longer required. Another interesting comparison is the overall stress response of *Pg* to different community members. In this study we found no significant transcriptional changes in either the general stress response or the oxidative stress response of *Pg*, despite the presence of oxygen during community development. In contrast, *Pg* stress responses were down-regulated in the presence of *Sg*, highlighting their strong physiological compatibility. One notable exception was the oxidative stress response genes which were up-regulated in the presence of *Sg*. These differences may highlight that as a strict aerobe, *Ab* unlike *Sg* may provide a strong oxidative protection to *Pg*. One common response of *Pg* to both *Ab* and *Sg* is the up-regulation of the T9SS. This secretion system functions in the export of key virulence determinants such as PPAD and the gingipain proteases. While the community-associated function of these diverse effectors are largely uncharacterized, the increased secretion of potential community effectors in response to polymicrobial environments may result in community-wide alterations that are hallmarks of the dysbiosis associated with *Pg* infection.

## Conclusion

Here we present a comprehensive transcriptional analysis of the key periodontal pathogen *Pg* and the opportunistic pathogen *Ab* as they sense and adapt to a heterotypic community. Model communities of *Pg* had greater numbers of bacteria in the presence of *Ab* compared to monotypic communities suggesting a synergistic relationship. Multiple adhesins were regulated by both *Pg* and *Ab* along with other biofilm associated factors. *Pg* and *Ab* showed synergistic metabolism in our model, and transcript levels of key virulence factors of both

organisms were up-regulated in the heterotypic communities suggesting potential synergistic pathogenicity. The results of this study suggest that *Pg* and *Ab* may physically interact with each other during human infection to increase fitness due to cooperative metabolism and community development as well as promote immune dysregulation by manipulating neutrophil recruitment. In this study, we describe the transcriptional responses of *Pg* and *Ab* to a dual species community and provide key insights into the interaction of these two important human pathogens. While the scope of this study was limited to identifying and describing these interactions at the transcriptional level, additional studies are required to elucidate the underlying mechanisms and to functionally characterize the interactions described here, and to determine to extent to which the results from this model are applicable to an *in vivo* setting. In particular, study of the role of metabolic mutualism, differential protein secretion, and capsule biosynthesis may provide novel insights into synergistic pathogenicity.

## Supplementary Material

Refer to Web version on PubMed Central for supplementary material.

## Acknowledgments

Supported by NIH/NIDCR DE012505 (RL), DE023193 (RL), DE026939 (DM) and DE018276 (AW). We thank Ashley Best for helpful advice.

## References

1. Darveau RP. Periodontitis: a polymicrobial disruption of host homeostasis. *Nat Rev Microbiol.* 2010; 8(7):481–490. [PubMed: 20514045]
2. Hajishengallis G, Lamont RJ. Dancing with the Stars: How choreographed bacterial interactions dictate nosymbiocity and give rise to keystone pathogens, accessory pathogens, and pathobionts. *Trends Microbiol.* 2016; 24(6):477–489. [PubMed: 26968354]
3. Lamont RJ, Hajishengallis G. Polymicrobial synergy and dysbiosis in inflammatory disease. *Trends Mol Med.* 2015; 21(3):172–183. [PubMed: 25498392]
4. Stacy A, McNally L, Darch SE, Brown SP, Whiteley M. The biogeography of polymicrobial infection. *Nat Rev Microbiol.* 2016; 14(2):93–105. [PubMed: 26714431]
5. Jenkinson HF, Lamont RJ. Oral microbial communities in sickness and in health. *Trends Microbiol.* 2005; 13(12):589–595. [PubMed: 16214341]
6. Rosan B, Lamont RJ. Dental plaque formation. *Microbes Infect.* 2000; 2(13):1599–1607. [PubMed: 11113379]
7. Atanasova KR, Yilmaz O. Prelude to oral microbes and chronic diseases: past, present and future. *Microbes Infect.* 2015; 17(7):473–483. [PubMed: 25813714]
8. Kumar PS. Oral microbiota and systemic disease. *Anaerobe.* 2013; 24:90–93. [PubMed: 24128801]
9. Maddi A, Scannapieco FA. Oral biofilms, oral and periodontal infections, and systemic disease. *Am J Dent.* 2013; 26(5):249–254. [PubMed: 24479275]
10. Okuda K, Kimizuka R, Abe S, Kato T, Ishihara K. Involvement of periodontopathic anaerobes in aspiration pneumonia. *J Periodontol.* 2005; 76(11 Suppl):2154–2160.
11. Whitmore SE, Lamont RJ. Oral bacteria and cancer. *PLoS Pathog.* 2014; 10(3):e1003933. [PubMed: 24676390]
12. da Silva-Boghossian CM, do Souto RM, Luiz RR, Colombo AP. Association of red complex, *A. actinomycetemcomitans* and non-oral bacteria with periodontal diseases. *Arch Oral Biol.* 2011; 56(9):899–906. [PubMed: 21397893]

13. Didilescu AC, Skaug N, Marica C, Didilescu C. Respiratory pathogens in dental plaque of hospitalized patients with chronic lung diseases. *Clin Oral Investig*. 2005; 9(3):141–147.
14. Watanabe K, Senba M, Ichinose A, Yamamoto T, Ariyoshi K, Matsumoto K. Bactericidal activity in filtrated supernatant of *Streptococcus sanguinis* against multidrug-resistant *Pseudomonas aeruginosa*. *J Exp Med*. 2009; 219(2):79–84.
15. Ali RW, Velcescu C, Jivanescu MC, Lofthus B, Skaug N. Prevalence of 6 putative periodontal pathogens in subgingival plaque samples from Romanian adult periodontitis patients. *J Clin Periodontol*. 1996; 23(2):133–139. [PubMed: 8849850]
16. Slots J, Rams TE, Feik D, Taveras HD, Gillespie GM. Subgingival microflora of advanced periodontitis in the Dominican Republic. *J Periodontol*. 1991; 62(9):543–547. [PubMed: 1658290]
17. Souto R, Silva-Boghossian CM, Colombo AP. Prevalence of *Pseudomonas aeruginosa* and *Acinetobacter* spp. in subgingival biofilm and saliva of subjects with chronic periodontal infection. *Braz J Microbiol*. 2014; 45(2):495–501. [PubMed: 25242933]
18. Richards AM, Abu Kwaik Y, Lamont RJ. Code blue: *Acinetobacter baumannii*, a nosocomial pathogen with a role in the oral cavity. *Mol Oral Microbiol*. 2015; 30(1):2–15. [PubMed: 25052812]
19. Colombo AP, Boches SK, Cotton SL, et al. Comparisons of subgingival microbial profiles of refractory periodontitis, severe periodontitis, and periodontal health using the human oral microbe identification microarray. *J Periodontol*. 2009; 80(9):1421–1432. [PubMed: 19722792]
20. Colombo AP, Haffajee AD, Dewhirst FE, et al. Clinical and microbiological features of refractory periodontitis subjects. *J Clin Periodontol*. 1998; 25(2):169–180. [PubMed: 9495617]
21. Scannapieco FA. Role of oral bacteria in respiratory infection. *J Periodontol*. 1999; 70(7):793–802. [PubMed: 10440642]
22. Hayes C, Sparrow D, Cohen M, Vokonas PS, Garcia RI. The association between alveolar bone loss and pulmonary function: the VA dental longitudinal study. *Ann Periodontol*. 1998; 3(1):257–261. [PubMed: 9722709]
23. Scannapieco FA, Bush RB, Paju S. Associations between periodontal disease and risk for nosocomial bacterial pneumonia and chronic obstructive pulmonary disease. A systematic review. *Ann Periodontol*. 2003; 8(1):54–69. [PubMed: 14971248]
24. Scannapieco FA, Ho AW. Potential associations between chronic respiratory disease and periodontal disease: analysis of National Health and Nutrition Examination Survey III. *J Periodontol*. 2001; 72(1):50–56. [PubMed: 11210073]
25. Bartlett JG, Gorbach SL, Finegold SM. The bacteriology of aspiration pneumonia. *Am J Med*. 1974; 56(2):202–207. [PubMed: 4812076]
26. Finegold SM, Strong CA, McTeague M, Marina M. The importance of black-pigmented gram-negative anaerobes in human infections. *FEMS Immunol Med Microbiol*. 1993; 6(2–3):77–82. [PubMed: 8518764]
27. Nelson S, Laughon BE, Summer WR, Eckhaus MA, Bartlett JG, Jakab GJ. Characterization of the pulmonary inflammatory response to an anaerobic bacterial challenge. *Am Rev Respir Dis*. 1986; 133(2):212–217. [PubMed: 3946920]
28. Kimizuka R, Kato T, Ishihara K, Okuda K. Mixed infections with *Porphyromonas gingivalis* and *Treponema denticola* cause excessive inflammatory responses in a mouse pneumonia model compared with mono-infections. *Microbes Infect*. 2003; 5(15):1357–1362. [PubMed: 14670448]
29. Pan Y, Teng D, Burke AC, Haase EM, Scannapieco FA. Oral bacteria modulate invasion and induction of apoptosis in HEp-2 cells by *Pseudomonas aeruginosa*. *Microb Pathogenesis*. 2009; 46(2):73–79.
30. Merritt J, Kreth J, Shi W, Qi F. LuxS controls bacteriocin production in *Streptococcus mutans* through a novel regulatory component. *Mol Microbiol*. 2005; 57(4):960–969. [PubMed: 16091037]
31. Adams MD, Goglin K, Molyneaux N, et al. Comparative genome sequence analysis of multidrug-resistant *Acinetobacter baumannii*. *J Bacteriol*. 2008; 190(24):8053–8064. [PubMed: 18931120]
32. Naito M, Hirakawa H, Yamashita A, et al. Determination of the genome sequence of *Porphyromonas gingivalis* strain ATCC 33277 and genomic comparison with strain W83 revealed

- extensive genome rearrangements in *P. gingivalis*. DNA Res. 2008; 15(4):215–225. [PubMed: 18524787]
33. Storey JD, Tibshirani R. Statistical significance for genomewide studies. Proc Natl Acad Sci U S A. 2003; 100(16):9440–9445. [PubMed: 12883005]
  34. Storey JD, Tibshirani R. Statistical methods for identifying differentially expressed genes in DNA microarrays. Methods Mol Biol. 2003; 224:149–157. [PubMed: 12710672]
  35. Huber W, Carey VJ, Gentleman R, et al. Orchestrating high-throughput genomic analysis with Bioconductor. Nat Methods. 2015; 12(2):115–121. [PubMed: 25633503]
  36. Kuboniwa M, Tribble GD, James CE, et al. *Streptococcus gordonii* utilizes several distinct gene functions to recruit *Porphyromonas gingivalis* into a mixed community. Mol Microbiol. 2006; 60(1):121–139. [PubMed: 16556225]
  37. Hendrickson EL, Beck DA, Miller DP, et al. Insights into dynamic polymicrobial synergy revealed by time-coursed RNA-Seq. Front Microbiol. 2017; 8:261. [PubMed: 28293219]
  38. Diaz PI, Slakeski N, Reynolds EC, Morona R, Rogers AH, Kolenbrander PE. Role of OxyR in the oral anaerobe *Porphyromonas gingivalis*. J Bacteriol. 2006; 188(7):2454–2462. [PubMed: 16547032]
  39. Teufel R, Mascaraque V, Ismail W, et al. Bacterial phenylalanine and phenylacetate catabolic pathway revealed. Proc Natl Acad Sci U S A. 2010; 107(32):14390–14395. [PubMed: 20660314]
  40. Bhuiyan MS, Ellett F, Murray GL, et al. *Acinetobacter baumannii* phenylacetic acid metabolism influences infection outcome through a direct effect on neutrophil chemotaxis. Proc Natl Acad Sci U S A. 2016; 113(34):9599–9604. [PubMed: 27506797]
  41. Cerqueira GM, Kostoulas X, Khoo C, et al. A global virulence regulator in *Acinetobacter baumannii* and its control of the phenylacetic acid catabolic pathway. J Infect Dis. 2014; 210(1):46–55. [PubMed: 24431277]
  42. Grenier D. Nutritional interactions between two suspected periodontopathogens, *Treponema denticola* and *Porphyromonas gingivalis*. Infect Immun. 1992; 60(12):5298–5301. [PubMed: 1333450]
  43. Garcia B, Olivera ER, Minambres B, et al. Phenylacetyl-coenzyme A is the true inducer of the phenylacetic acid catabolism pathway in *Pseudomonas putida*. Appl Environ Microbiol. 2000; 66(10):4575–4578.
  44. Lamont RJ, Jenkinson HF. Subgingival colonization by *Porphyromonas gingivalis*. Oral Microbiol Immun. 2000; 15(6):341–349.
  45. Lamont RJ, Jenkinson HF. Life below the gum line: pathogenic mechanisms of *Porphyromonas gingivalis*. Microbiol Mol Biol Rev. 1998; 62(4):1244–1263. [PubMed: 9841671]
  46. Nishiyama S, Murakami Y, Nagata H, Shizukuishi S, Kawagishi I, Yoshimura F. Involvement of minor components associated with the FimA fimbriae of *Porphyromonas gingivalis* in adhesive functions. Microbiol. 2007; 153(Pt 6):1916–1925.
  47. Belanger M, Kozarov E, Song H, Whitlock J, Progulske-Fox A. Both the unique and repeat regions of the *Porphyromonas gingivalis* hemagglutinin A are involved in adhesion and invasion of host cells. Anaerobe. 2012; 18(1):128–134. [PubMed: 22100486]
  48. Hasegawa Y, Nagano K, Ikai R, et al. Localization and function of the accessory protein Mfa3 in *Porphyromonas gingivalis* Mfa1 fimbriae. Mol Oral Microbiol. 2013; 28(6):467–480. [PubMed: 24118823]
  49. Ikai R, Hasegawa Y, Izumigawa M, et al. Mfa4, an accessory protein of Mfa1 Fimbriae, modulates fimbrial biogenesis, cell auto-aggregation, and biofilm formation in *Porphyromonas gingivalis*. PLOS One. 2015; 10(10):e0139454. [PubMed: 26437277]
  50. Eijkelkamp BA, Stroehrer UH, Hassan KA, Paulsen IT, Brown MH. Comparative analysis of surface-exposed virulence factors of *Acinetobacter baumannii*. BMC Genomics. 2014; 15:1020. [PubMed: 25422040]
  51. Rumbo-Feal S, Gomez MJ, Gayoso C, et al. Whole transcriptome analysis of *Acinetobacter baumannii* assessed by RNA-sequencing reveals different mRNA expression profiles in biofilm compared to planktonic cells. PLOS One. 2013; 8(8):e72968. [PubMed: 24023660]

52. Eijkelkamp BA, Hassan KA, Paulsen IT, Brown MH. Investigation of the human pathogen *Acinetobacter baumannii* under iron limiting conditions. *BMC Genomics*. 2011; 12:126. [PubMed: 21342532]
53. Tomaras AP, Dorsey CW, Edelmann RE, Actis LA. Attachment to and biofilm formation on abiotic surfaces by *Acinetobacter baumannii*: involvement of a novel chaperone-usher pili assembly system. *Microbiol*. 2003; 149(12):3473–3484.
54. Lee JC, Koerten H, van den Broek P, et al. Adherence of *Acinetobacter baumannii* strains to human bronchial epithelial cells. *Res Microbiol*. 2006; 157(4):360–366. [PubMed: 16326077]
55. Marti S, Nait Chabane Y, Alexandre S, et al. Growth of *Acinetobacter baumannii* in pellicle enhanced the expression of potential virulence factors. *PLOS One*. 2011; 6(10):e26030. [PubMed: 22046254]
56. Pukatzki S, McAuley SB, Miyata ST. The type VI secretion system: translocation of effectors and effector-domains. *Curr Opin Microbiol*. 2009; 12(1):11–17. [PubMed: 19162533]
57. Sana TG, Lugo KA, Monack DM. T6SS: The bacterial “fight club” in the host gut. *PLOS Pathogen*. 2017; 13(6):e1006325. [PubMed: 28594921]
58. Repizo GD, Gagne S, Foucault-Grunewald ML, et al. Differential role of the T6SS in *Acinetobacter baumannii* virulence. *PLOS One*. 2015; 10(9):e0138265. [PubMed: 26401654]
59. Ruiz FM, Santillana E, Spinola-Amilibia M, Torreira E, Culebras E, Romero A. Crystal structure of Hcp from *Acinetobacter baumannii*: A component of the Type VI secretion system. *PLOS One*. 2015; 10(6):e0129691. [PubMed: 26079269]
60. Silverman JM, Brunet YR, Cascales E, Mougous JD. Structure and regulation of the type VI secretion system. *Annu Rev Microbiol*. 2012; 66:453–472. [PubMed: 22746332]
61. Weber BS, Hennon SW, Wright MS, et al. Genetic dissection of the Type VI secretion system in *Acinetobacter* and identification of a novel peptidoglycan hydrolase, TagX, required for its biogenesis. *mBio*. 2016; 7(5)
62. Chen WJ, Kuo TY, Hsieh FC, et al. Involvement of type VI secretion system in secretion of iron chelator pyoverdine in *Pseudomonas taiwanensis*. *Sci Rep*. 2016; 6:32950. [PubMed: 27605490]
63. Gallique M, Bouteiller M, Merieau A. The Type VI secretion system: A dynamic system for bacterial communication. *Front Microbiol*. 2017; 8:1454. [PubMed: 28804481]
64. Burtnick MN, Brett PJ, Harding SV, et al. The cluster 1 type VI secretion system is a major virulence determinant in *Burkholderia pseudomallei*. *Infect Immun*. 2011; 79(4):1512–1525. [PubMed: 21300775]
65. Ma AT, Mekalanos JJ. In vivo actin cross-linking induced by *Vibrio cholerae* type VI secretion system is associated with intestinal inflammation. *Proc Natl Acad Sci U S A*. 2010; 107(9):4365–4370. [PubMed: 20150509]
66. Lasica AM, Ksiazek M, Madej M, Potempa J. The Type IX secretion system (T9SS): Highlights and recent insights into its structure and function. *Front Cell Infect Microbiol*. 2017; 7:215. [PubMed: 28603700]
67. Kadowaki T, Yukitake H, Naito M, et al. A two-component system regulates gene expression of the type IX secretion component proteins via an ECF sigma factor. *Sci Rep*. 2016; 6:23288. [PubMed: 26996145]
68. Guo Y, Nguyen KA, Potempa J. Dichotomy of gingipains action as virulence factors: from cleaving substrates with the precision of a surgeon’s knife to a meat chopper-like brutal degradation of proteins. *Periodontol 2000*. 2010; 54(1):15–44. [PubMed: 20712631]
69. Goulas T, Mizgalska D, Garcia-Ferrer I, et al. Structure and mechanism of a bacterial host-protein citrullinating virulence factor, *Porphyromonas gingivalis* peptidylarginine deiminase. *Sci Rep*. 2015; 5:11969. [PubMed: 26132828]
70. Gully N, Bright R, Marino V, et al. *Porphyromonas gingivalis* peptidylarginine deiminase, a key contributor in the pathogenesis of experimental periodontal disease and experimental arthritis. *PLOS One*. 2014; 9(6):e100838. [PubMed: 24959715]
71. O’Brien-Simpson NM, Paolini RA, Hoffmann B, Slakeski N, Dashper SG, Reynolds EC. Role of RgpA, RgpB, and Kgp proteinases in virulence of *Porphyromonas gingivalis* W50 in a murine lesion model. *Infect Immun*. 2001; 69(12):7527–7534. [PubMed: 11705929]

72. Bielecka E, Scavenius C, Kantyka T, et al. Peptidyl arginine deiminase from *Porphyromonas gingivalis* abolishes anaphylatoxin C5a activity. *J Biol Chem*. 2014; 289(47):32481–32487. [PubMed: 25324545]
73. Potempa J, Nguyen KA. Purification and characterization of gingipains. *Curr Protoc Protein Sci*. 2007; Chapter 21(Unit 21.20)
74. Zhou Y, Sztukowska M, Wang Q, et al. Noncanonical activation of beta-catenin by *Porphyromonas gingivalis*. *Infect Immun*. 2015; 83(8):3195–3203. [PubMed: 26034209]
75. Barth K, Genco CA. Microbial degradation of cellular kinases impairs innate immune signaling and paracrine TNFalpha responses. *Sci Rep*. 2016; 6:34656. [PubMed: 27698456]
76. Kesavalu L, Holt SC, Ebersole JL. Trypsin-like protease activity of *Porphyromonas gingivalis* as a potential virulence factor in a murine lesion model. *Microb Pathogenesis*. 1996; 20(1):1–10.
77. Kondo Y, Ohara N, Sato K, et al. Tetratricopeptide repeat protein-associated proteins contribute to the virulence of *Porphyromonas gingivalis*. *Infect Immun*. 2008; 78:2846–2856.
78. Kenyon JJ, Hall RM. Variation in the complex carbohydrate biosynthesis loci of *Acinetobacter baumannii* genomes. *PLOS One*. 2013; 8(4):e62160. [PubMed: 23614028]
79. Russo TA, Luke NR, Beanan JM, et al. The K1 capsular polysaccharide of *Acinetobacter baumannii* strain 307-0294 is a major virulence factor. *Infect Immun*. 2010; 78(9):3993–4000. [PubMed: 20643860]
80. Wu X, Chavez JD, Schweppe DK, et al. In vivo protein interaction network analysis reveals porin-localized antibiotic inactivation in *Acinetobacter baumannii* strain AB5075. *Nat Commun*. 2016; 7:13414. [PubMed: 27834373]
81. Lewis JP. Metal uptake in host-pathogen interactions: role of iron in *Porphyromonas gingivalis* interactions with host organisms. *Periodontol 2000*. 2010; 52(1):94–116. [PubMed: 20017798]
82. Smalley JW, Olczak T. Haem acquisition mechanisms of *Porphyromonas gingivalis* - strategies used in polymicrobial community in a haem-limited host environment. *Mol Oral Microbiol*. 2015
83. Scott JC, Klein BA, Duran-Pinedo A, Hu L, Duncan MJ. A two-component system regulates heme acquisition in *Porphyromonas gingivalis*. *PLOS One*. 2013; 8(9):e73351. [PubMed: 24039921]
84. Olczak T, Simpson W, Liu X, Genco CA. Iron and heme utilization in *Porphyromonas gingivalis*. *FEMS Microbiol Rev*. 2005; 29(1):119–144. [PubMed: 15652979]
85. Slakeski N, Dashper SG, Cook P, Poon C, Moore C, Reynolds EC. A *Porphyromonas gingivalis* genetic locus encoding a heme transport system. *Oral Microbiol Immun*. 2000; 15(6):388–392.
86. Gao JL, Nguyen KA, Hunter N. Characterization of a hemophore-like protein from *Porphyromonas gingivalis*. *J Biol Chem*. 2010; 285(51):40028–40038. [PubMed: 20940309]

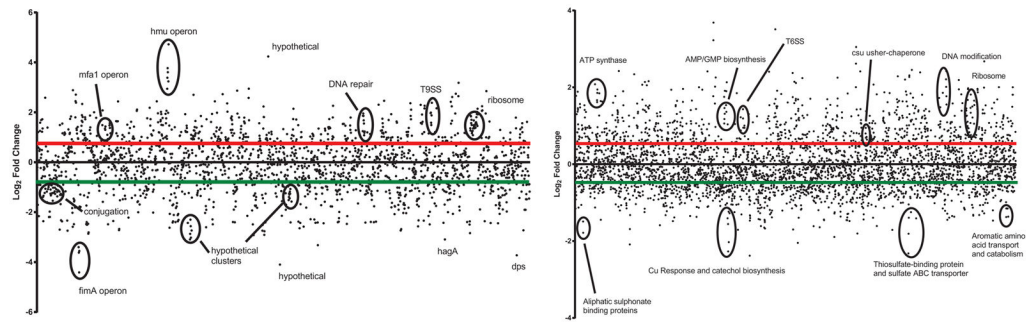


**Figure 1. Dot graph of DE genes and functional clusters**

Each dot represents the transcriptional response of every ORF numbered sequentially moving from left to right in *PgAb* vs *Pg* (left) and *PgAb* vs *Ab* (right). The red and green bars represent the significance cutoffs of 0.5 and  $-0.5 \log_2$  fold change, respectively.



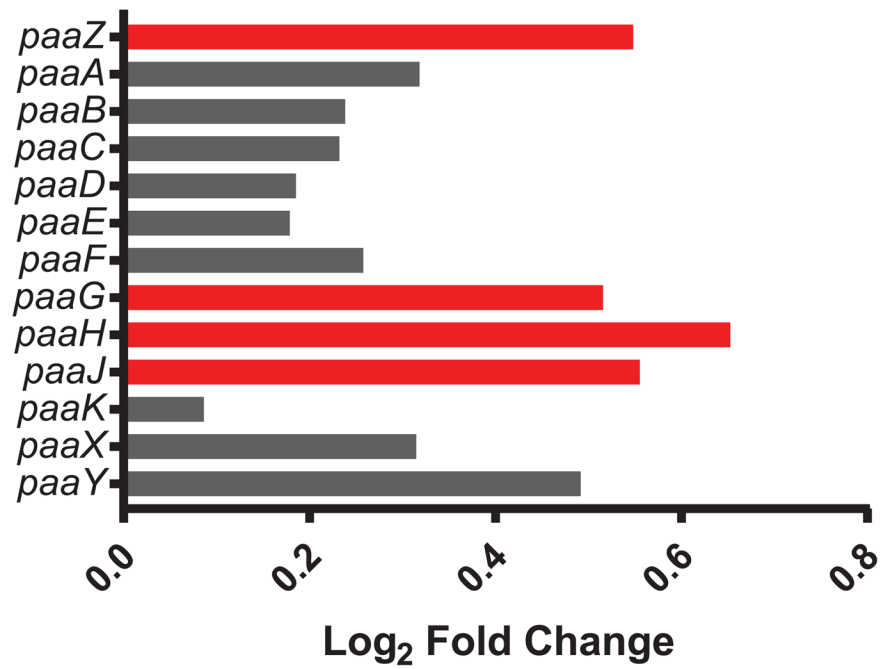


**Figure 2. Differential expression of genes within the phenylacetic acid catabolism pathway in the *PgAb* communities compared to *Ab* alone**

Results are expressed as log<sub>2</sub> fold change in the *PgAb* community compared to *Ab* alone. Higher mRNA levels are represented as red bars and those with no significant change are shown as gray.

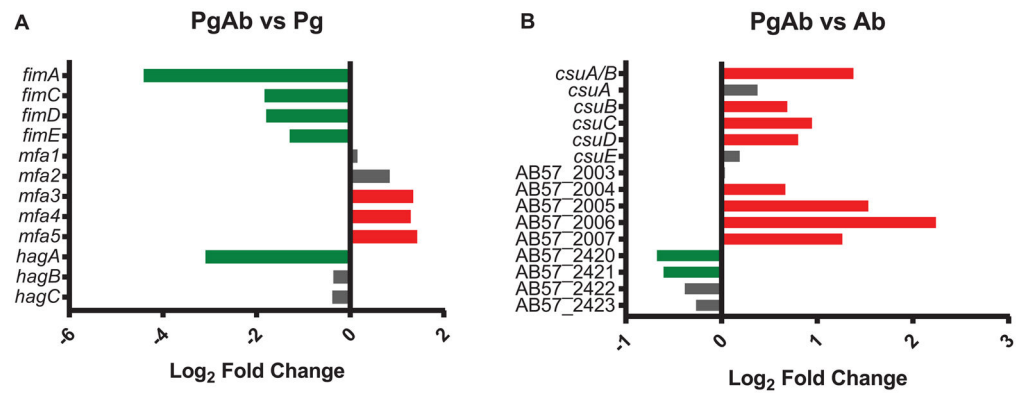


**Figure 3. Differential expression of adhesins in the *PgAb* communities**

Results are expressed as  $\log_2$  fold change in the *PgAb* community compared to *Pg* (A) or *Ab* (B) alone. Higher mRNA levels are represented as red bars, lower levels are represented as green bars and those with no significant change are shown as gray.

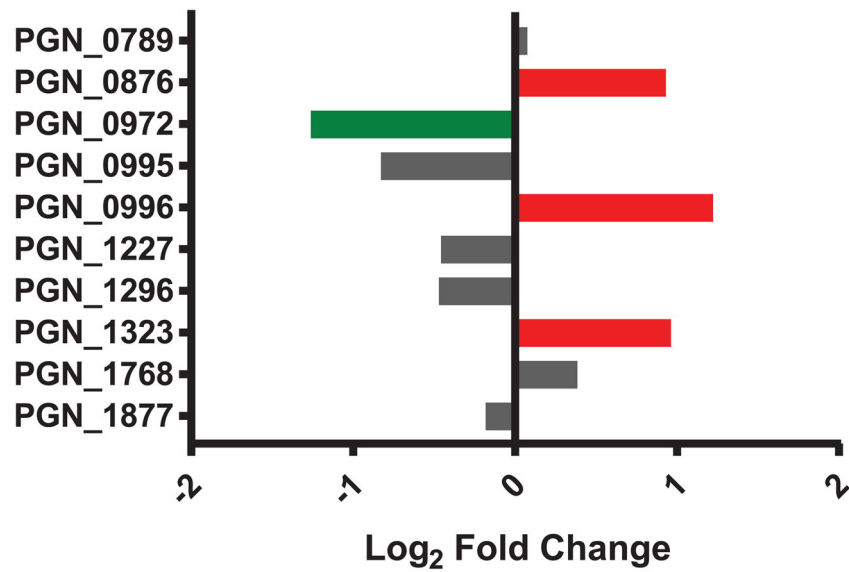


**Figure 4. Differential expression of *Pg* TPR domain containing proteins in the *PgAb* communities**  
Results are expressed as log<sub>2</sub> fold change in the *PgAb* community compared to *Pg* alone.  
Higher mRNA levels are represented as red bars, lower expression is represented as green bars and those with no significant change are shown as gray.

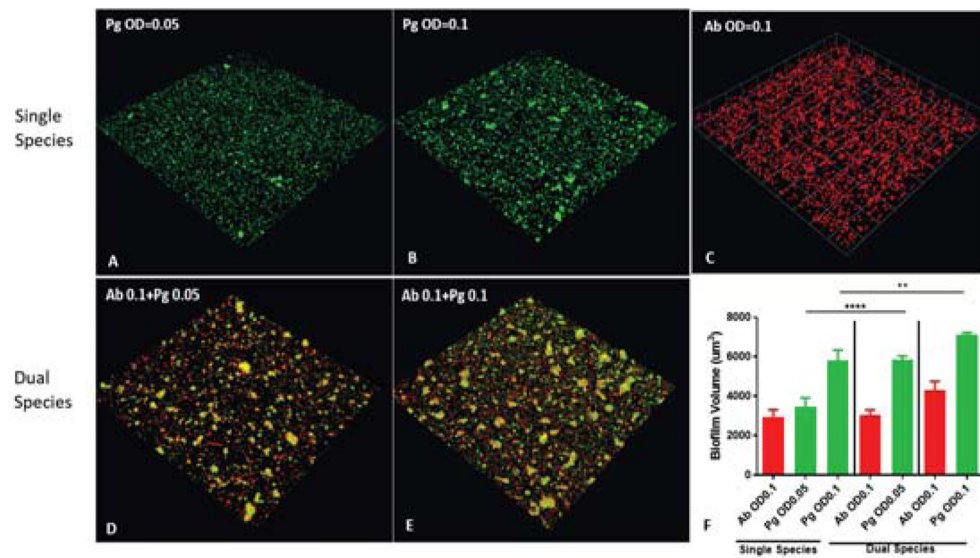


**Figure 5. *Ab* enhances *Pg* community development**

(A–E) *Pg* (green) was incubated alone or reacted with a substratum of *Ab* (red) for 16 h at the cell densities indicated. A series of x-y sections were collected by confocal microscopy and digitally reconstructed into a three-dimensional image. Images are representative of 3 independent experiments. (F) Calculated biovolume of *Pg* and *Ab* in the images represented in (A–E) measured using the Volocity software. Results are means with standard deviation of the three experiments. \*\* $P < 0.01$ , \*\*\*\*  $P < 0.0001$  compared between *PgAb* and *Pg* alone using ANOVA with Tukey's multiple comparison test.

**Table 1**Pathway analysis of Ab genes differentially expressed in *PgAb* communities

Pathway Name	Genes UP	Genes DOWN	FDR <sup>I</sup>
Aminoacyl-tRNA biosynthesis	27	1	6.31E-06
One carbon pool by folate	11	1	0.000476599
Fatty acid biosynthesis	13	1	0.000569961
Sulfur metabolism	14	16	0.001322774
Pyrimidine metabolism	36	2	0.001330085
Glycine, serine and threonine metabolism	24	8	0.002933338
Lysine biosynthesis	12	4	0.006448065
Purine metabolism	47	21	0.007516597
Phenylalanine, tyrosine and tryptophan biosynthesis	21	2	0.008386424
Peptidoglycan biosynthesis	18	1	0.008877038
Fructose and mannose metabolism	8	2	0.011766396
Cysteine and methionine metabolism	21	8	0.011981639
Methane metabolism	15	4	0.013718309
Vitamin B6 metabolism	5	1	0.013718309
Novobiocin biosynthesis	4	0	0.025871218
Arginine and proline metabolism	12	5	0.025871218
Propanoate metabolism	27	10	0.030004433
Pyruvate metabolism	29	13	0.030004433
Biotin metabolism	10	3	0.030004433
Amino sugar and nucleotide sugar metabolism	14	5	0.035195636
Oxidative phosphorylation	35	4	0.04482427
Folate biosynthesis	11	8	0.04482427
Tyrosine metabolism	6	8	0.04482427
Arginine biosynthesis	11	9	0.047789592

<sup>I</sup> Pathway analysis was performed using the Bioconductor package and pathways were considered significant with a false-discovery rate (FDR) < 0.05

**Table 2**Differential expression of *Ab* genes associated with the type 6 secretion system in *PgAb* communities

Gene Name	Gene Name	log <sub>2</sub> Fold Change <sup>1</sup>	Product
AB57_1158		0.36272	Rhs element Vgr protein, putative
AB57_1442		0.18630	putative VGR-related protein
AB57_1479	tssB	1.4309	type VI secretion protein, family
AB57_1480	tssC	1.19192	type VI secretion protein, EvpB/family
AB57_1481	Hcp	0.79672	type VI secretion system effector, Hcp1 family
AB57_1482	tssE	0.94882	type VI secretion system lysozyme-related protein
AB57_1483	tssF	0.3391	type VI secretion protein, family
AB57_1484	tssG	-0.28688	type VI secretion protein, family
AB57_1485		-0.69577	hypothetical protein
AB57_1486	tssM	0.31656	type VI secretion protein IcmF
AB57_1487	tagF	0.393	type VI secretion-associated protein, family
AB57_1488	tagN	0.31515	OmpA/MotB domain protein
AB57_1489	PAAR Class I	-0.12307	hypothetical protein
AB57_1490	clpV	0.45938	type VI secretion ATPase, ClpV1 family
AB57_1491	tssA	1.00499	type VI secretion-associated protein, ImpA family
AB57_1492	tssK	0.94866	type VI secretion protein, family
AB57_1493	tssL	0.52583	type IV / VI secretion system protein, DotU family
AB57_1494		0.72873	hypothetical protein
AB57_1495	tagX	0.53119	D-alanyl-D-alanine carboxypeptidase family
AB57_3817		0.96823	putative VGR-related protein

<sup>1</sup>Results are expressed as log<sub>2</sub> fold change in *PgAb* compared to *Ab* alone. Higher mRNA levels are represented as red and statistically unchanged are in black.

**Table 3**

Differential expression of Pg genes associated with the type 9 secretion system machinery, regulation and the C-terminal domain containing cargo proteins

PGN Number	Product	Log2 Fold Change <sup>I</sup>
T9SS Machinery		
PGN_0022	porU	1.2229
PGN_0023	porV	1.7245
PGN_0274	SigP	0.8691
PGN_0297	conserved hypothetical protein	0.2566
PGN_0300	conserved hypothetical protein	0.0084
PGN_0509	porZ	0.778
PGN_0645	porQ	0.4576
PGN_0778	porT	0.5775
PGN_0832	sov	1.3021
PGN_1019	porX	-0.5066
PGN_1235	porS	0.9197
PGN_1236	porR	1.4053
PGN_1296	putative OmpA family protein	-0.4692
PGN_1437	conserved hypothetical protein	-0.4112
PGN_1673	porN	1.9698
PGN_1674	porM	1.9886
PGN_1675	porL	1.5849
PGN_1676	porK	1.4903
PGN_1677	porP	1.8791
PGN_1877	porW	-0.1808
PGN_2001	porY	-0.2595
T9SS Cargo Proteins		
PGN_0022	Por secretion system protein porU	1.2229
PGN_0123	conserved hypothetical protein	-1.1650
PGN_0152	immunoreactive 61 kDa antigen	-2.0225
PGN_0291	accessory fimbrial protein, Mfa5	1.4341
PGN_0335	conserved hypothetical protein	0.5009
PGN_0509	immunoreactive 84 kDa antigen	0.7780
PGN_0561	trypsin like proteinase PrtT	1.4692
PGN_0654	conserved hypothetical protein	-2.8665
PGN_0657	conserved hypothetical protein	-3.0214
PGN_0659	35 kDa hemin binding protein	0.9471
PGN_0693	conserved hypothetical protein	0.5442
PGN_0795	conserved hypothetical protein	0.5725
PGN_0810	conserved hypothetical protein	2.3564
PGN_0852	immunoreactive 47 kDa antigen	2.8683

PGN Number	Product	Log2 Fold Change <sup>1</sup>
PGN_0898	peptidylarginine deiminase PPAD	1.0088
PGN_0900	thiol protease	2.5795
PGN_1115	putative hemagglutinin	-2.6414
PGN_1321	conserved hypothetical protein	-2.1576
PGN_1416	probable lysyl endopeptidase precursor	-0.5973
PGN_1466	arginine-specific cysteine proteinase RgpB	1.0239
PGN_1476	conserved hypothetical protein	2.4632
PGN_1556	conserved hypothetical protein	-2.0303
PGN_1611	leucine-rich domain protein, InlJ	0.0975
PGN_1728	lysine-specific cysteine proteinase Kgp	0.0043
PGN_1733	hemagglutinin protein HagA	-3.0918
PGN_1767	immunoreactive 46 kDa antigen	-2.0675
PGN_1770	conserved hypothetical protein	0.2688
PGN_1790	arginine-specific cysteine proteinase RgpA	-0.458
PGN_2065	putative Lys- and Rgp- gingipain domain protein	-2.7273
PGN_2080	conserved hypothetical protein	1.6173

<sup>1</sup>Results are expressed as log<sub>2</sub> fold change in *PgAb* compared to *Pg* alone. Higher mRNA levels are represented as red, lower levels are represented as green, and statistically unchanged are in black.

Author Manuscript

Author Manuscript

Author Manuscript

Author Manuscript



**Table 4**Differential expression of *Ab* genes associated with capsule biosynthesis and transport

Gene ID	Product	log <sub>2</sub> Fold Change <sup>1</sup>
AB57_0090	peptidyl-prolyl cis-trans isomerase Mip	0.08133
AB57_0091	tyrosine-protein kinase ptk	0.90987
AB57_0092	protein-tyrosine-phosphatase ptp	0.71925
AB57_0093	polysaccharide export protein	0.54358
AB57_0094	VI polysaccharide biosynthesis protein VipA/tviB	1.35879
AB57_0095	VI polysaccharide biosynthesis protein VipB/tviC	1.34966
AB57_0096	polysaccharide biosynthesis protein	0.08478
AB57_0097	hypothetical protein	0.54264
AB57_0098	hypothetical protein	-0.1949
AB57_0099	glycosyl transferase, group 1	-0.35419
AB57_0100	hypothetical protein	-0.31633
AB57_0101	hypothetical protein	-0.47685
AB57_0102	putative glycosyl transferase family 1	0.32779
AB57_0103	glycosyl transferase, group 1	-0.06922
AB57_0104	UDP-glucose 4-epimerase	0.5243
AB57_0105	polyprenol phosphate:N-acetyl-hexosamine 1-phosphate transferase	0.95193
AB57_0106	acetyltransferase	0.3451
AB57_0107	nucleotide sugar epimerase/dehydratase	0.46067
AB57_0108	UDP-glucose 4-epimerase	0.7211
AB57_0109	hypothetical protein	-0.4545
AB57_0110	acyltransferase	-0.27185
AB57_0111	UTP-glucose-1-phosphate uridylyltransferase	-0.14983
AB57_0112	NDP-sugar dehydrogenase	-0.13951
AB57_0113	glucose-6-phosphate isomerase	0.1811
AB57_0114	UDP-glucose 4-epimerase	0.14976
AB57_0115	phosphomannomutase	0.4157
AB57_0116	L-lactate permease	0.67559
AB57_1078	hypothetical protein, wzi homolog	0.99645

<sup>1</sup>Results are expressed as log<sub>2</sub> fold change in *PgAb* compared to *Ab* alone. Higher mRNA levels are represented as red, lower levels are represented as green, and statistically unchanged are in black.

**Table 5**Differential expression of heme and iron acquisition genes in the *PgAb* communities compared to *Pg* alone

<b><i>PgAb</i> vs <i>Pg</i></b>		
Gene ID	Product	Log <sub>2</sub> Fold Change <sup>1</sup>
PGN_0553	hmuV	3.3866
PGN_0554	hmuU	3.7695
PGN_0555	hmuT	3.6057
PGN_0556	hmuS	1.9810
PGN_0557	hmuR	3.2401
PGN_0558	humY	4.7244
PGN_0604	ferritin	-2.0719
PGN_0659	35 kDa heme binding protein	0.9471
PGN_0683	thr	-1.2954
PGN_0684	htrD	-1.3200
PGN_0685	htrC	-1.2234
PGN_0686	htrB	-1.2209
PGN_0687	htrA	-1.1410
PGN_0704	ihtA	0.4271
PGN_0705	ihtB	0.0173
PGN_0706	ihtC	0.7127
PGN_0707	ihtD	0.4343
PGN_0708	ihtE	0.6481
PGN_0752	haeS	-1.7992
PGN_0753	haeR	-1.5937
PGN_1058	bcp	-1.7021
PGN_1085	feoB	0.0982
PGN_1087		1.3151
PGN_1335		1.7903
PGN_1336		1.1816
PGN_1503	furR	0.1741
PGN_2037	dps	-3.7272
PGN_2090	husB	-0.8785
PGN_2091	husA	-1.1772

<sup>1</sup>Results are expressed as log<sub>2</sub> fold change in *PgAb* compared to *Pg* alone. Higher mRNA levels are represented as red, lower levels are represented as green, and statistically unchanged are in black.